Available online at www.sciencedirect.com
ScienceDirect
Analytical Biochemistry 373 (2008) 197–206
ANALYTICAL BIOCHEMISTRY
www.elsevier.com/locate/yabio

Staurosporine-based binding assay for testing the affinity of compounds to protein kinases

Ganesh H. Iyer, Paul Taslimi, S. Pazhanisamy *

Vertex Pharmaceuticals Incorporated, Cambridge, MA 02139, USA

Received 12 July 2007
Available online 20 December 2007

Abstract

Staurosporine is a broad-spectrum inhibitor of both tyrosine and serine/threonine protein kinases. Excitation of staurosporine and its analogues at 296 nm results in major emission bands centered at 378 and 396 nm. The intensity of the emission bands is enhanced on binding to the adenosine triphosphate (ATP) site of many protein kinases. This property was used to develop a competitive displacement assay for evaluating the binding affinity of small molecules to protein kinases. The assay was validated in both cuvette and plate formats for several phosphorylated and non-phosphorylated protein kinases. The throughput of the assay is high enough to be used in drug discovery for screening as well as lead optimization.

Keywords: Staurosporine; Binding assay; Competitive ligand displacement; Fluorescence; Dissociation constant; Protein kinase

Protein kinases constitute an important class of enzymes engaged in intracellular signaling via cascades of interconnected biochemical pathways. There are well over 500 protein kinases in the human genome, and their post-translational activities are further modulated by more than 100 phosphatases [1]. Aberrant kinase activities have been linked to many diseases, ranging from cancer to inflammation to central nervous system (CNS)[1] diseases. Therefore, the human kinome offers a wealth of targets for drug discovery [2–6]. Over a decade and a half, a number of in vitro biochemical assays were developed to screen compounds for their potency against protein kinases [7,8]. Most of these assays measure the inhibition constant, K_i, of the compound by monitoring the decrease of kinase activity as a function of the test compound concentration. Intense activity in the kinase arena has resulted in the discovery of potent inhibitors for a number of therapeutic targets; many have advanced to human testing, and a few have already been approved as drugs [4]. Nearly all of the small molecule drug candidates in development block adenosine triphosphate (ATP) binding to the kinase as their primary mode of action.

While inhibition of the activated kinase (usually phosphorylated at the activation loop) was used in the optimization of binding potency, X-ray crystallographic analysis of cocomplex structure of inhibitors at the active site of the non-phosphorylated kinase often has been used in the inhibitor design process. Atomic-level structure data for the phosphorylated protein is not always available. In most cases, it is hard to obtain a large quantity of homogeneous phosphorylated protein. X-ray crystallographic observations indicate that the non-phosphorylated and phosphorylated proteins crystallize in "open" and "closed" conformations, respectively, with some exceptions [9,10]. There is accumulating evidence that the activated (phosphorylated) kinases adopt very similar conformations,

* Corresponding author. Fax: +1 617 444 6105.
E-mail address: pazhanisamy@vrtx.com (S. Pazhanisamy).

[1] *Abbreviations used:* CNS, central nervous system; ATP, adenosine triphosphate; ITC, isothermal calorimetry; SPR, surface plasmon resonance; FP, fluorescence polarization; TR–FRET, time-resolved Förster resonance energy transfer; ANS, 1-anilinonaphthalene-8-sulfonate; MAPKAP K-2, mitogen-activated protein kinase-associated protein kinase-2; Lck, leukocyte kinase; Src, src kinase; DMSO, dimethyl sulfoxide; DTT, dithiothreitol; TNF-α, tumor necrosis factor-α; IL-1β, interleukin 1β; CV, coefficient of variation.

0003-2697/$ - see front matter © 2007 Elsevier Inc. All rights reserved.
doi:10.1016/j.ab.2007.11.004

whereas the non-phosphorylated kinases sample distinct conformational spaces within the open conformation [11]. Hence, one school of thought is that greater selectivity can be achieved by targeting non-phosphorylated proteins. Glivec, for example, preferentially binds to an inactive form of c-Abl [12]. Because most non-phosphorylated proteins have low or no measurable kinase activity, biophysical methods must be used to measure the binding affinity of the compounds.

There are a number of assays described in the literature for the evaluation of the dissociation constant, K_d, for small molecule binding to protein. Among them, isothermal calorimetry (ITC) [13], capillary electrophoresis [14], and equilibrium dialysis [15] are not practical if throughput is one of the desired features of the assay. Surface plasmon resonance (SPR) [16] is amenable to higher throughput. However, it is a heterogeneous assay requiring immobilization of protein; therefore, the assay development may be potentially time-consuming. There is the additional concern that the immobilization process might alter the affinity of the ligand. Fluorescence techniques also are commonly used in binding studies [17]. Quenching of the intrinsic fluorescence of tryptophan and/or tyrosine residues of the protein on binding of a small molecule can be exploited in such assays. However, not all protein–ligand interactions lead to protein fluorescence quenching; hence, it is not a universal method.

Another commonly employed method for determining the K_d value is the competitive displacement assay. Radioactivity [18], prompt fluorescence [19], fluorescence polarization (FP) [20], and time-resolved Förster resonance energy transfer (TR–FRET) [21] are some of the detection methods used in the competitive displacement assay. The radioactivity-based assay requires separation of the protein-bound radioligand from the unbound, whereas the other assays are of the "mix and read" type. The TR–FRET assay can be carried out with a small quantity of protein; however, it requires specially engineered antibodies, boosting the cost of the assay. Fluorescent dyes such as 1-anilinonaphthalene-8-sulfonate (ANS) that bind to hydrophobic pockets often have been used to explore the binding of compounds [22,23]. A major disadvantage of this method is that the dye might not necessarily bind at the active site of the enzyme. As a result, the dye might not sense the small molecule binding at the active site, which is the primary target site for potential drug design.

Here we report a competitive displacement assay that is based on the prompt fluorescence of staurosporine, a broad-spectrum inhibitor of both serine and tyrosine protein kinases. Staurosporine is a well-characterized ATP competitive inhibitor of numerous protein kinases.[2] A number of crystal structures have been solved for staurosporine-bound protein kinases, confirming the binding to be at the ATP pocket [24]. Staurosporine absorbs at 296 nm and exhibits major emission bands centered at 378 and 396 nm (Fig. 1). The intensity of the emission bands is enhanced in hydrophobic environments such as 2-octanol and binding at the active site of a protein. The broad-spectrum activity of staurosporine coupled with its favorable fluorescence properties makes it a good reporter ligand (hereafter called a probe) to develop a competitive ligand displacement assay. Here we describe the development and validation of the binding assay with staurosporine and its analogues using a number of phosphorylated and non-phosphorylated protein kinases. The assay has been implemented in 96- and 384-well plate formats to rapidly evaluate compounds in the drug discovery paradigm.

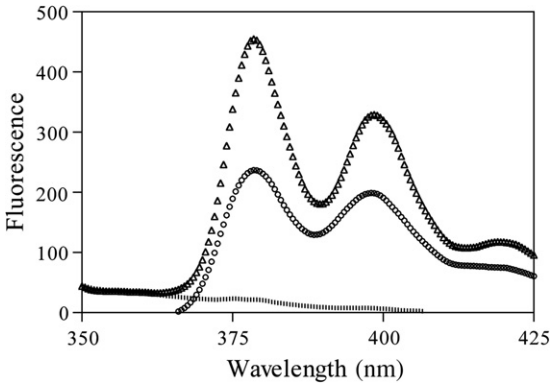

Fig. 1. Emission spectrum of staurosporine in the presence and absence of MAPKAP K-2. On excitation at 296 nm, the emission spectrum of 0.5 μM staurosporine in 500 μl of buffer (25 mM Hepes [pH 7.5], 10 mM $MgCl_2$, and 2% DMSO) shows two bands centered at 378 and 396 nm (o). The addition of 0.5 μM MAPKAP K-2 to 0.5 μM staurosporine leads to enhanced emission at those bands (Δ). In the absence of staurosporine, 0.5 μM MAPKAP K-2 in buffer (|) did not have a significant contribution to either of those bands.

Materials and methods

Reagents

Staurosporine and its analogues K252 (a and b) were purchased from Sigma Chemical (St. Louis, MO, USA). The small molecule inhibitors used in this study are proprietary compounds of Vertex Pharmaceuticals (Cambridge, MA, USA). The protein kinases mitogen-activated protein kinase-associated protein kinase-2 (MAPKAP K-2), leukocyte kinase (Lck), and src kinase (Src) were full-length recombinant proteins expressed and purified at Vertex Pharmaceuticals according to our previously published procedure [25].

Titrations in cuvette

A PerkinElmer LS-50B spectrofluorimeter (Boston, MA, USA) was used for the cuvette-based titrations. In a typical experiment, 500 μl of buffer (25 mM Hepes [pH

[2] The Kinase Profiler brochure from Upstate Biotechnology (Lake Placid, NY, USA) reports that at 1 μM concentration, staurosporine inhibited more than 80% of the activity among 72 of the 84 protein kinases, including serine/threonine and tyrosine kinases, when tested in the presence of 10 μM ATP.

7.5], 10 mM $MgCl_2$, and 2% dimethyl sulfoxide [DMSO]) containing 0.5 μM staurosporine was placed in a quartz cuvette equipped with a stir bar and was kept at constant stirring. Small aliquots (1–2 μl) of 28 μM activated MAPKAP K-2 in buffer (25 mM Hepes [pH 7.4], 50 mM NaCl, 2 mM dithiothreitol [DTT], and 5% glycerol) were added. The excitation and emission slit-widths were set at 10 and 3 nm, respectively. After each addition, an emission spectrum was obtained from 320 to 450 nm on excitation at 296 nm. The intensity of emission at 378 nm (or 396 nm) as a function of the MAPKAP K-2 was fitted to Eq. (1) (see Results and Discussion) to obtain the dissociation constant, K_d. The fluorescence enhancement observed at 378 nm for staurosporine (or its analogue) bound to Src or Lck is roughly twice that for MAPKAP K-2-bound staurosporine. Hence, for Lck and Src titrations, the protein and staurosporine concentrations were reduced in half.

To investigate the K_d value of a compound by the competitive displacement method, 500 μl of buffer (described above) containing 0.92 μM staurosporine (or its analogue) and 0.84 μM MAPKAP K-2 was placed in a cuvette, maintaining constant stirring. Compound addition and spectral recordings were carried out as before. The decrease in fluorescence intensity at 378 nm as a function of the added compound concentration was fitted to Eq. (4) (see Results and Discussion) to evaluate the K_d value.

Titrations in plate

Fluorescence measurements were carried out on a SpectraMax Gemini plate reader from Molecular Devices (Sunnyvale, CA, USA) using a black 96-well plate (Corning, NY, USA). For the determination of staurosporine K_d, buffer (described above) containing 0.67 μM staurosporine was placed 150 μl per well in 10 wells. To each well, 50 μl of either buffer alone or buffer containing kinase at different concentrations was added and mixed. The samples were excited at 296 nm, and the emission readings at 378 nm (top read) were noted. The data were processed as described above for the cuvette-based assays.

For the compound assay, staurosporine (or its analogue) and protein were premixed at 0.90 and 0.88 μM, respectively, and distributed 200 μl per well. Compound in DMSO at various concentrations was added at a volume of 1.5 μl per well and mixed. The fluorescence emission at 378 nm was measured before and after the addition of compound. The difference yielded the decrease in fluorescence as a function of the concentration of the compound. The data were fitted to Eq. (4) to evaluate the K_d value.

Screening compounds

The compound screening for the activated Src was carried out in 96-well plates using K252a as the reporter ligand. First, to each well, 200 μl of buffer containing K252a (0.5 μM) and activated Src (0.44 μM) was distributed. The fluorescence intensity at 378 nm (F_{EK}) was noted. Then 1.5 μl of compound in DMSO (5 μM final) was added and mixed, and the fluorescence reading (F_{EKC}) was taken. In a separate well, K252a alone in buffer containing the same volume of DMSO was added, and the fluorescence reading was noted (F_K). From these readings, fractional displacement of K252a from the complex, F_D, was calculated according to Eq. (5) (see Results and Discussion). A compound with $F_D \geqslant 0.35$, which corresponds to a K_d value $\leqslant 2$ μM, was considered a hit. (See the next section for details.)

Results and discussion

Fluorescence property of staurosporine and its analogues

Staurosporine is a complex natural product with a bisindole maleimide core (Fig. 2). It exhibits an absorption band centered at 296 nm, which is far enough from the absorption wavelengths of tyrosine and tryptophan to have any interference from the protein. There are two prominent emission bands centered at 378 and 396 nm (Fig. 1) for staurosporine that are well removed from the protein fluorescence. Staurosporine binding at the ATP site of MAPKAP K-2 resulted in roughly a 40% increase in intensity at 378 nm, the band that is most sensitive of the two emission bands (Fig. 1). Similar increases in intensities (35–70%) have been observed with the serine/threonine protein kinases ROCK I [26] and GSK3 (data not shown) and the tyrosine kinases Src and Lck (this work). There are a number of staurosporine analogues available, including K252 (a, b, and c), KT5720, and KT5823 (Fig. 2), which exhibit similar fluorescence properties (data not shown). These analogues, however, might potentially differ in binding affinity for any given kinase. Therefore, it should be possible to find a staurosporine analogue whose binding affinity for the protein kinase of interest matches that of the test compound to serve as a sensitive reporter ligand in the competitive ligand binding assay. Below we discuss more on how to select the proper reporter ligand.

Binding affinity to MAPKAP-2

MAPKAP K-2 is a substrate of p38, a key MAP kinase implicated in the transduction of pro-inflammatory signals [27]. Blockade of MAPKAP K-2 activation leads to a reduction in the concentration of the pro-inflammatory cytokines tumor necrosis factor-α (TNF-α) and interleukin 1β (IL-1β). Therefore, MAPKAP K-2 is of considerable interest as a target for drug discovery. We used activated MAPKAP K-2 to validate the competitive displacement binding assay. Initially, a cuvette-based binding assay was established with staurosporine. The successive addition of activated MAPKAP K-2 to staurosporine in buffer resulted in an increase in fluorescence intensity at 378 nm. The increase in emission intensity at 378 nm as a function of MAPKAP K-2 concentration (Fig. 3) was fitted to Eq. (1) [26] to obtain the dissociation constant, K_d. E_0, L_0, and $\Delta\varepsilon$ are the protein concentration, ligand concentration,

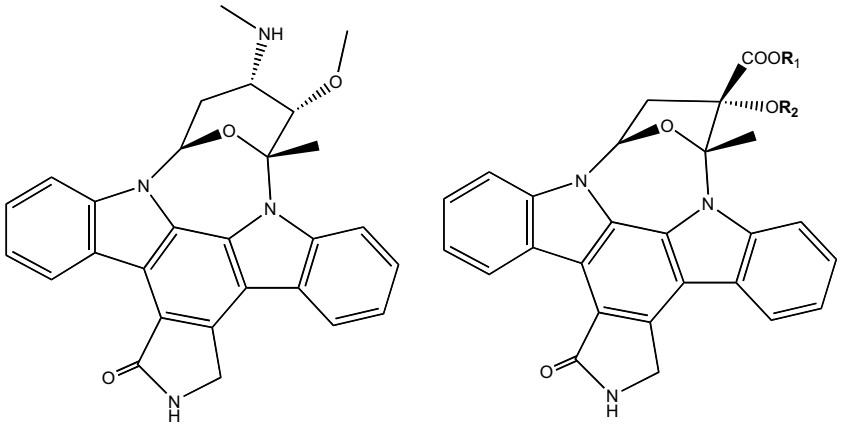

Staurosporine Staurosporine analogue

Substitution	K-252a	K-252b	KT-5823	KT-5720
$\mathbf{R_1}$	CH_3	H	CH_3	$(CH_2)_5$-CH_3
$\mathbf{R_2}$	H	H	CH_3	H

Fig. 2. Structure of staurosporine and its analogues.

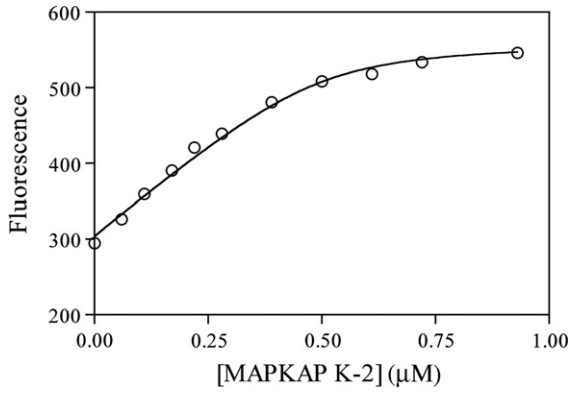

Fig. 3. Titration of staurosporine with activated MAPKAP K-2. In a quartz cuvette, 500 μM buffer (25 mM Hepes [pH 7.5], 10 mM $MgCl_2$, and 2% DMSO) containing 0.5 μM staurosporine was placed. To this, concentrated solution of activated MAPKAP K-2 (28 μM) was added 1 μl at a time. The increase in emission intensity at 378 nm, on excitation at 296 nm, was plotted as a function of the MAPKAP K-2 concentration. The best fit curve shown was obtained using Eq. (1).

and increase in molar emissivity for staurosporine on binding to protein, respectively. An average K_d value of 38 ± 10 nM (Table 1) was obtained for staurosporine. In the 96-well plate format, staurosporine titrations yielded an average K_d value of 36 ± 20 nM, which is in very good agreement with the cuvette assay. We also titrated K252a and K252b in the 96-well plate and obtained values of 22 ± 14 and 670 ± 280 nM, respectively (Table 1). Thus, staurosporine and its analogues do exhibit a wide range of K_d values for the same protein kinase.

$$\Delta F = (\Delta\varepsilon/2)\left[(K_d + E_0 + L_0) - \sqrt{(K_d + E_0 + L_0)^2 - 4E_0L_0}\right]. \quad (1)$$

Table 1
Dissociation constants for inhibitors of MAPKAP K-2

Compound	K_i (nM)	K_d (nM)[a]	
		Cuvette	96-well plate
A	5 ± 1	3 ± 1	3.6 ± 3.0
B	67 ± 6	31 ± 6	25 ± 11
C	138 ± 23	308 ± 62	239 ± 28
Staurosporine	31 ± 7	38 ± 10	36 ± 20
K252a	–	–	22 ± 14
K252b	620 ± 80	–	670 ± 280

[a] The values reported for K_i and K_d are based on a minimum of three replicates.

Competitive ligand displacement assay

In the competitive ligand displacement assay, two compounds (a probe such as staurosporine or its analogue and the test compound) compete for binding to the same protein (Eq. (2)). Let the nominal concentration of protein, probe, and ligand in the assay be $[P]_0$, $[R]_0$, and $[L]_0$, respectively. Let the dissociation constants for the probe and the ligand be K_{d1} and K_{d2}, respectively. The concentration of protein-bound probe, $[PR]$, at any given condition can be obtained from Eq. (3), which is an exact solution originally derived by Wang [28].

$$[\text{Kinase. Staurosporine}] \overset{K_{d1}}{\leftrightarrow} \text{Kinase} \overset{K_{d2}}{\leftrightarrow} [\text{Kinase. Compound}] \quad (2)$$

$$[PR] = \frac{[R]_0\{2\sqrt{(a^2 - 3b)}\cos(\theta/3) - a\}}{3k_{d1} + \{2\sqrt{(a^2 - 3b)}\cos(\theta/3) - a\}}, \quad (3)$$

where

$$a = K_{d1} + K_{d2} + [R]_0 + [L]_0 - [P]_0$$
$$b = K_{d2}([R]_0 - [P]_0) + K_{d1}([L_0] - [P_0]) + K_{d1}K_{d2}$$
$$c = -K_{d1}K_{d2}[P_0]$$
$$\theta = \arccos\frac{-2a^3+9ab-27c}{2\sqrt{(a^2-3b)^3}}.$$

In principle, competitive displacement titrations may be set up by one of three ways: (i) varying the protein concentration, (ii) varying the ligand concentration, or (iii) varying the probe concentration while keeping the concentration of the other two agents constant. Varying the probe concentration is less desirable for the following reasons. First, the total fluorescence due to the probe increases linearly with its concentration, whereas the fraction of the total probe that is bound to the protein decreases at high concentrations, making it difficult to accurately estimate the net increase in fluorescence due to binding in the background of high fluorescence. Second, the inner filter effect and solubility of the probe will limit the titration at high concentrations. To appreciate the difference between the "ligand concentration variation" and "protein concentration variation" methods, simulations were carried out to understand the behavior of the titration curves as a function of the characteristics of the components in the assay.

Simulation of titration curves for varying the ligand concentration

In this method, the probe and the protein are premixed, to which the ligand is added incrementally. The initial fluorescence will be at a maximum because the protein-bound probe concentration is the highest in the absence of the competitor. The addition of ligand leads to a decrease in signal as it displaces the probe from the protein. The signal intensity, F, is given by Eq. (4), where $\Delta\varepsilon$ is the increase in molar extinction coefficient for the probe on binding to the protein and F_0 is probe fluorescence in the absence of protein. The expression for $[PR]$ is obtained from Eq. (3). In all of the simulations, a value of 500 U was used for $\Delta\varepsilon$, which was close to the observed value in the plate assay. Also, it was assumed that the protein and the ligand do not contribute significantly to the emission.[3] The steepness of the titration curve is a function of the dissociation constants for the probe and the ligand, as illustrated by the simulated curves in Fig. 4. The protein and probe concentrations were kept equal to 1 μM. The K_d for the probe was 20 nM for the simulation of data in Fig. 4A and 200 nM in Fig. 4B. Titration curves were generated for ligands with K_d values ranging from 1 to 1000 nM. Although the inflexion points were well separated from each other for the curves in Figs. 4A and 4B, the resolution was much better between the curves in Fig. 4A than in Fig. 4B. In reality, the titration curve will have far fewer data points than the simulation, and the associated experimental error will present a further challenge to estimating the K_d of the test compound. Therefore, a probe with a K_d value closer to 20 nM is likely better able to differentiate compounds of varying affinities than is the one with a K_d value of a few hundred nanomolar. However, ligands approaching a K_d value of 1 μM exhibit more curvature, with the probe having a K_d value of 200 nM (Fig. 4B). Therefore, ideally the probe and the ligand should have similar affinities for the protein to yield the best titration curve. At the same time, a higher K_d value for the probe means a smaller fraction of bound species to begin with (for a given concentration of protein) and, hence, a smaller window of signal for the titration. In a screening campaign, compounds of differing affinities will be assayed with a single probe. Therefore, a probe with optimal affinity to discriminate compounds of various potencies should be identified. From the simulations, it appears that a probe with a K_d value of 20 to 50 nM will be a reasonable choice.

$$F = F_0 + \Delta\varepsilon[PR]. \quad (4)$$

We also simulated conditions where the protein and probe concentrations were not equal (Figs. 4C and 4D). When the protein concentration was half that of the probe, the dynamic range of the change in fluorescence was reduced accordingly (Fig. 4C). However, keeping the protein concentration twice that of the probe had a dramatic effect on the shape of the titration curve (Fig. 4D). The curves were sigmoidal, and the sigmoidicity increased as the affinity of the ligand increased for the protein. The sigmoidicity stems from the fact that at low concentrations the test ligand finds enough free protein to bind without needing to displace probe from its complex. In a real titration with far fewer data points, this shape may be either missed or easily mistaken for lack of data quality. Therefore, maintaining the protein concentration equal to, or somewhat less than, that of the probe will ensure the maximum signal without the added complexity.

Simulation of titration curves for varying the protein concentration

Keeping both the probe and the test ligand at a fixed concentration and titrating in the protein, in principle, can give a higher dynamic range compared with the case where the test ligand was varied [19]. The increase in fluorescence, $F - F_0$, will be directly proportional to the protein-bound staurosporine (Eq. 4, $[PR]$ as defined in Eq. (3)) and should reach up to the same maximum value at high protein concentration for every compound. However, there may be practical limitations to going too high in protein concentration. In the simulations, we considered two different concentrations of test ligand: (i) the ligand and

[3] None of the proteins used in this study had any significant fluorescence at 378 nm. Some compounds used in the screen (Table 2) had fluorescence at 378 nm in a concentration-dependant manner. In those cases, the compound fluorescence was subtracted to get the change in fluorescence due to the displacement of the probe.

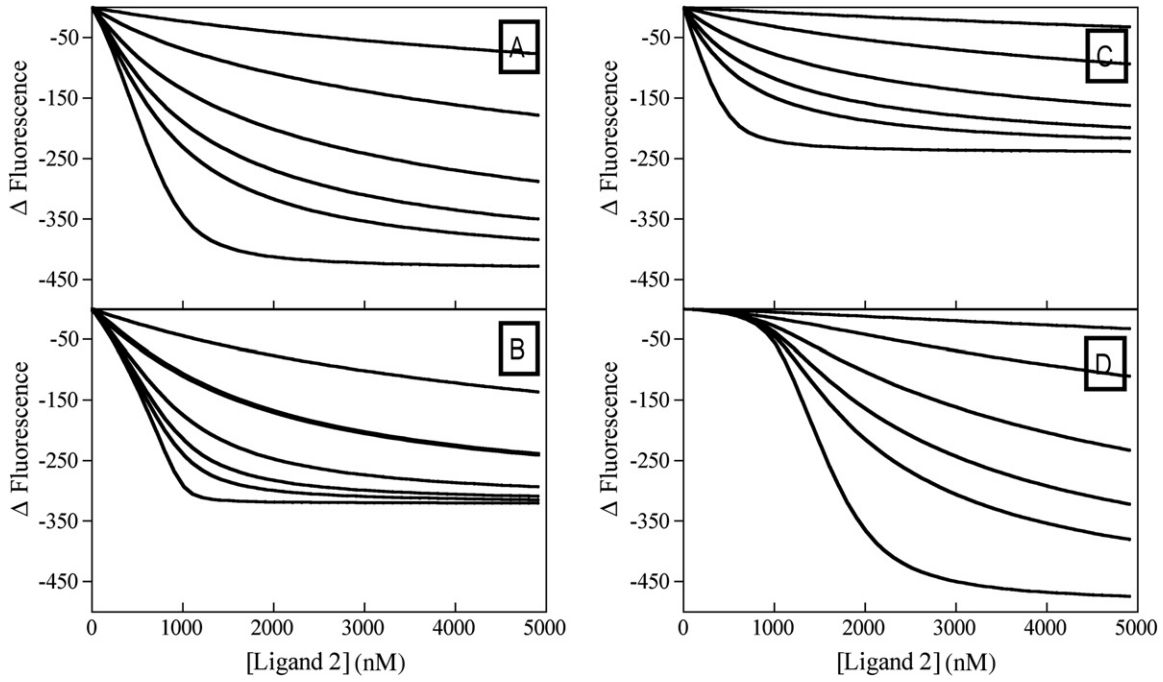

Fig. 4. Simulated data for the decrease in fluorescence as a function of test ligand concentration. Eq. (4) was used for the simulations. Increase in molar extinction coefficient was assumed to be 500 U/μM probe–protein complex. Total probe concentration in the cuvette was 1 μM in all simulations. Its K_d value varied for each panel of simulations as given. (A) $[P]_0 = 1$ μM, $K_{d1} = 20$ nM. (B) $[P]_0 = 1$ μM, $K_{d1} = 200$ nM. (C) $[P]_0 = 0.5$ μM, $K_{d1} = 20$ nM. (D) $[P]_0 = 2$ μM, $K_{d1} = 20$ nM. In all panels, the K_d values of test ligand (K_{d2}) were 1, 10, 20, 50, 200, and 1000 nM, respectively, for the six curves from bottom to top.

probe concentrations were equal (1 μM) (Figs. 5A–5C) and (ii) the ligand was fivefold in excess (5 μM) over probe (1 μM) (Figs. 5D–5F). Again, test ligands with a range of affinities ($K_d = 1$–1000 nM) were considered for three different probe affinities ($K_d = 20$, 50, and 200 nM).

For any given K_d value of probe, the titration curves for compounds of various affinities were better separated if the test ligand was at a higher concentration than that of probe. However, this also required titrating in a fairly high concentration of protein to capture a reasonable portion of the titration curve. A striking feature of this method was that the increase in fluorescence intensity appeared to be fairly linear over a large portion of the titration if the affinities of the probe and test ligand were nearly equal. A convex curve resulted if the test ligand was weaker than the probe, whereas a concave curve (sigmoidal curve or lag) resulted if the test ligand was of higher affinity. Therefore, by visual inspection of the titration curve, one can get a feel for the relative binding potency of the test ligand compared with the probe. From the different affinities of the probes considered, a K_d value of approximately 50 nM for the probe may be optimal to discriminate the test ligands of a wide range of affinities.

Although this method offers some unique advantages over the ligand variation method, it requires at least twofold more protein. This could be a deciding factor if a large number of titrations were to be carried out. As a result, in the examples to follow, we used the ligand variation method to validate the assay.

Titration of MAPKAP K-2 inhibitors in the cuvette

Three ATP-competitive inhibitors of MAPKAP K-2 with K_i values spanning low nanomoles to micromoles were used to establish the assay. MAPKAP K-2 (0.5 μM) and staurosporine (0.45 μM) were premixed to 500 μl in buffer (25 mM Hepes [pH 7.5] containing 2% DMSO and 10 mM $MgCl_2$) in a quartz cuvette. The test compound in DMSO was added 0.5 μl at a time. For each addition, the emission intensity at 378 nm was noted for the excitation at 296 nm. The fluorescence intensity was plotted as a function of the test ligand concentration (Fig. 6). The data were fitted to Eq. (4) to evaluate the dissociation constant. The K_d value obtained for each compound by this method was compared against its enzymatic K_i value in Table 1. The K_d values are within threefold of the K_i values. Both the K_i and K_d values refer to the dissociation constant for the compound from the protein, with one being obtained from activity inhibition assay and the other being obtained from binding assay. Differences between the measured dissociation constants due to the change in assay methodologies are well documented [29,30], and the two- to threefold variations are well within the accepted range.

Validation of plate assay

To be useful as a tool for drug discovery, the assay should have a reasonable throughput. We first tried a 96-well plate format of the competitive displacement assay.

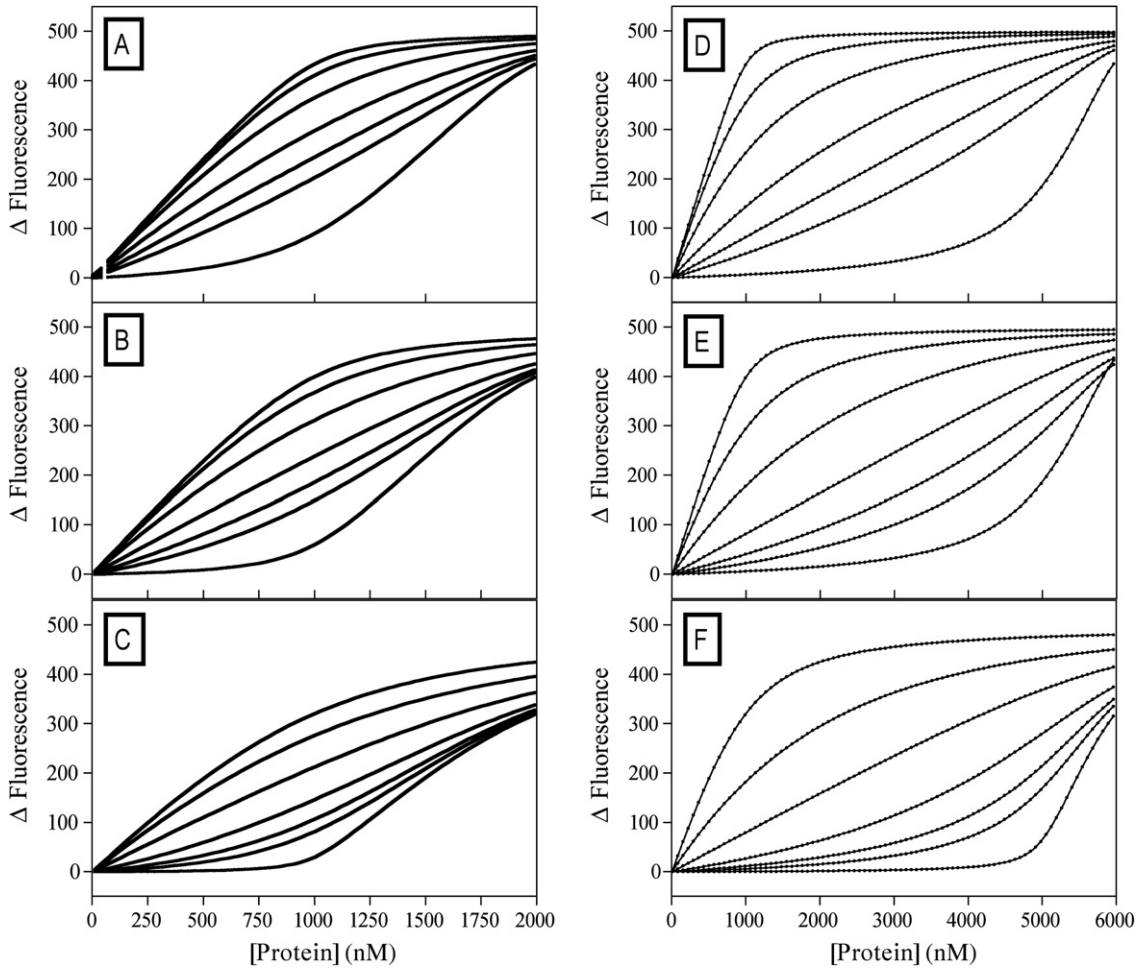

Fig. 5. Simulated data for the increase of fluorescence as a function of the protein concentration. Eq. (4) was used for the simulations. Probe concentration was constant at 1 μM in all simulations. The test ligand (ligand 2) was kept at 1 μM in panels A to C and at 5 μM in panels D to F. Probe K_d (K_{d1}) was 20 nM for panels A and D, 50 nM for panels B and E, and 200 nM for panels C and F. The top curve in all of the panels represents titration in the absence of the test ligand. The curves below it (from top to bottom) represent titration in the presence of test ligand with K_d values (K_{d2}) of 1000, 200, 50, 20, 10, and 1 nM, respectively.

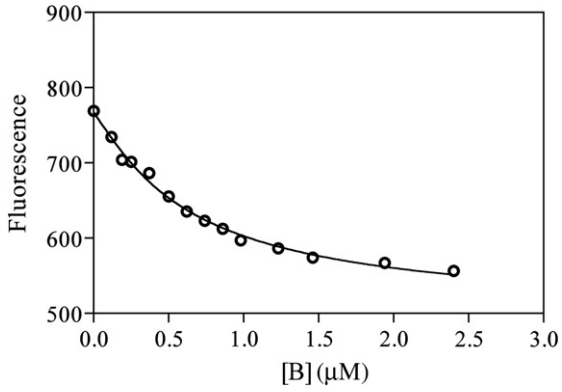

Fig. 6. Displacement of staurosporine with MAPKAP K-2 inhibitor. In a quartz cuvette, 500 μl of buffer (25 mM Hepes [pH 7.5], 10 mM $MgCl_2$, and 2% DMSO) containing 0.9 μM staurosporine and 0.8 μM activated MAPKAP K-2 was added. To this, DMSO solution of MAPKAP K-2 inhibitor was added in small aliquots (0.2–1 μl) at a time. The decrease in emission intensity at 378 nm for the excitation at 296 nm was plotted as a function of compound B concentration. The best fit curve shown was obtained by fitting the data to Eq. (4).

The same set of compounds and activated MAPKAP K-2 used in the cuvette assay were employed to validate the 96-well plate assay. Activated MAPKAP K-2 and staurosporine (or its analogue) were premixed and aliquotted 200 μl per well into 8 to 10 wells (2% DMSO). The fluorescence intensity at 378 nm was read for all of the wells. A 2-μl aliquot of compound in DMSO was added to each well and mixed, and the fluorescence reading was taken. The decrease in fluorescence readings for each well (difference between the pre- and postcompound addition readings) is plotted against the concentration of the compound. The data were analyzed by fitting to Eq. (4). The K_d values obtained by the plate assay agreed quite well with the cuvette data (Table 1) for all three compounds. We reproduced this assay in 384-well plates with an assay volume of 50 μl (data not shown). The Z factor [31] and coefficient of variation (CV) for the plate assays (for both 96- and 384-well formats) were 0.7 and 3%, respectively.

One advantage of the binding assay is that the protein need not have enzyme activity. We exploited this aspect

to compare the binding constant of a number of inhibitors, including staurosporine analogues, binding to both phosphorylated and non-phosphorylated Lck (data not shown). K252a, for example, binds to non-phosphorylated Lck with a K_d of 130 nM. Staurosporine, on the other hand, binds non-phosphorylated Lck very tightly with a low nanomolar K_d value. In the K_d determination assay, both the staurosporine and protein concentrations should be approximately 0.3 μM to yield a good signal. At this concentration, the titration with non-phosphorylated Lck yielded a rectangular hyperbola with a sharp curvature (Fig. 7A). Fitting the data to the quadratic equation (Eq. (1)) yielded a K_d value of 4.5 ± 1.3 nM. Often the curve fitting of such data either is not possible or presents a large error in the estimated K_d value. To get a better estimate of the K_d, we deliberately added a known concentration (1 μM) of a "silent" inhibitor whose K_d (20 nM) for non-phosphorylated Lck was obtained previously by competitive titration with K252a. A silent inhibitor is one that does not interfere with the absorbance or fluorescence of the probe but competes for binding to the active site of the kinase. In the presence of the silent inhibitor, the apparent K_d for staurosporine increased, resulting in a more shallow titration curve (Fig. 7B) and allowing a more reliable curve fitting. Fitting the data to Eq. (4) (apply Eq. (3) for $[PR]$), using the K_d and concentration of the silent inhibitor, yielded a value of 2.2 ± 0.7 nM for the K_d of staurosporine. Thus, a potent reporter ligand whose K_d value cannot be measured by direct titration can be determined in the presence of a silent competitive inhibitor of known K_d. In turn, using such tight binding reporter ligands, compounds with even lower K_d values can be evaluated.

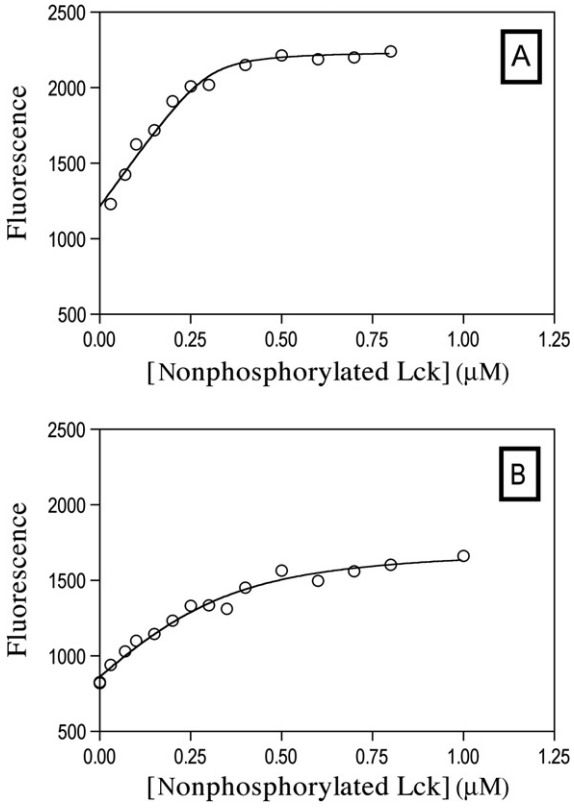

Fig. 7. Titration of staurosporine with non-phosphorylated Lck. (A) In a 96-well plate, 200 μM buffer (25 mM Hepes [pH 7.5], 10 mM $MgCl_2$, and 2% DMSO) containing 0.3 μM staurosporine was added to 10 wells. To each well, 1 μl of non-phosphorylated Lck of various concentrations was added to yield a final concentration of 0.0 to 0.8 μM. The increase in emission intensity at 378 nm, on excitation at 296 nm, was plotted as a function of the Lck concentration. The best fit curve shown was obtained using Eq. (1). (B) The titration was carried out as above except to include 1 μM of the silent inhibitor with a K_d value of 20 nM. The data were fit to Eq. (4).

Dissociation constant for ATP

The dissociation constant, K_d, for ATP cannot be assumed to be the same as K_m unless the phosphate transfer step is slow compared with the ATP binding step. The competitive displacement assay with staurosporine is ideal for obtaining the K_d of ATP. If there is any ATPase activity associated with the kinase, the cuvette assay might not be suitable because the incremental addition of ATP requires a reasonable length of time to complete the titration, resulting in significant hydrolysis of ATP. In the plate assay, each well receives a different concentration of ATP and, hence, the titration takes less time to complete. Also, adding ATP last can further minimize the contact time between ATP and protein. Using K252a as reporter ligand, we measured the K_d value for ATP binding to activated Lck as 143 ± 33 μM, which is similar to the K_m value of 118 ± 8 μM.

Screening compounds

Can this binding assay be used to screen a library of compounds? To explore this potential, we screened a test set of compounds against activated Src. We picked 24 compounds with K_i values in the range of nanomoles to high micromoles. K252a was used as the probe. Each compound was screened at 5 μM in duplicate. First, to each well, 200 μl of buffer containing K252a (0.5 μM) and activated Src (0.44 μM) was distributed. The fluorescence intensity at 378 nm (F_{EK}) was noted. Then 1.5 μl of compound in DMSO was added and mixed, and the fluorescence reading (F_{EKC}) was taken. In a separate well, K252a alone in buffer containing the same volume of DMSO was added, and the fluorescence reading (F_K) was noted. The fraction of K252a displaced (F_D) from Src was calculated from Eq. (5). Table 2 lists the F_D value for each compound along with its K_i value obtained previously from the kinase inhibition assay. We set the criterion of an F_D value of $\geqslant 0.35$ for a hit, corresponding to a predicted K_d value of $\leqslant 2$ μM.

$$F_D = \frac{(F_{EK} - F_{EKC})}{(F_{EK} - F_K)}. \quad (5)$$

Compounds 1 to 13 are hits in this assay, in agreement with the prediction based on the K_i values. However, compounds **14** to **16** and **18** have F_D values <0.35, whereas

Table 2
Screening compounds as binders of Src by competitive displacement of K252a

Compound	Fraction probe displaced[a] (F_D)	Hit[b]	K_i (μM)	K^d (μM)
1	1.21	Yes	0.01	0.3[c]
2	0.96	Yes	0.02	
3	0.84	Yes	0.02	0.2[c]
4	0.82	Yes	0.8	0.8
5	0.64	Yes	0.5	1.2
6	0.58	Yes	0.4	
7	0.52	Yes	0.01	
8	0.52	Yes	0.2	0.3
9	0.49	Yes	0.5	
10	0.42	Yes	0.2	0.3
11	0.41	Yes	0.6	0.4
12	0.37	Yes	0.6	
13	0.34	Yes	1.9	
14	0.26	No	**1.0**	1.2[d]
15	0.24	No	**1.5**	
16	0.22	No	**0.8**	0.4[d]
17	0.20	No	>4	
18	0.19	No	**0.6**	0.9[d]
19	0.18	No	>4	
20	0.15	No	>4	
21	−0.10	No	>4	
22	−0.16	No	>4	
23	−0.16	No	>4	
24	−0.35	No	2.6	

[a] Calculated according to Eq. (5).
[b] Defined as an F_D value $\geqslant 0.35$, which corresponds to a predicted $K_d \leqslant 2$ μM.
[c] The compound interferes with staurosporine fluorescence.
[d] The compound fluorescence subtracted to get a good fit of the data.

their K_i values are $\leqslant 2$ μM. One reason for this discrepancy may be that these compounds had significant fluorescence at 378 nm, leading to lower F_D values and, thus, an underestimation of their K_D values. Indeed, the above compounds had significant fluorescence (data not shown) when tested at 5 μM. We obtained a titration curve for these compounds and corrected for the background fluorescence before fitting the data. The K_d values obtained in this way were in good agreement with the K_i values. We also titrated some of the hits identified in the screen (Table 2) to obtain the K_d values. Some of the hits also had significant fluorescence warranting correction. After subtracting out the compound fluorescence, the data yielded K_d values that were similar to the K_i values. The K_d values of compounds 1 and 3 are higher than their respective K_i values by at least 10-fold. Both of these compounds interact with K252a, lowering its fluorescence; therefore, the titrations were less reliable. Hence, there is potential for false negatives if the compounds also absorb and/or emit at 296 and 378 nm, respectively.

Conclusion

The prompt fluorescence-based competitive binding assays reported in the literature for kinases were narrow in scope because the probes were designed to bind specific kinases [32]. The broad-spectrum inhibitory nature of staurosporine and its analogues makes this assay broadly applicable to kinases. The fluorescence intensity of staurosporine increases modestly ($\leqslant$ two-fold) on binding to protein; however, the increase was sufficient to follow the binding titration. This assay is amenable to high-throughput (96- and 384-well plate) formats and offers reliable K_d values, albeit requiring correction for compound fluorescence in some instances. The enzyme concentration in this assay is 0.3 to 0.5 μM, which is comparable to or less than that used in the binding assays such as ITC and protein fluorescence quenching. FP, TR–FRET, and enzyme fragment complementation assays [33] use less protein but require specifically modified probes and, therefore, could take a considerable lead time to develop the assays. This staurosporine-based assay is easy to develop and requires no further chemical modification. It is amenable to higher throughput in 96- and 384-well formats to minimize protein use. The availability of staurosporine analogues with similar fluorescence properties but with a range of affinities is an added feature. Also, this assay is suitable for obtaining K_d values for nucleotides binding to protein kinases. This assay naturally opens up the possibility to study compound binding to inactive (or low-activity) protein kinases. It is particularly useful for evaluating the constructs designed for X-ray crystallography where truncations or the phosphorylation state might have altered the enzyme activity. Retention of binding affinity for the putative kinase inhibitors is a prerequisite to ensure a cocomplex crystal, and therefore this binding assay should be useful to crystallographers working with ATP site inhibitors.

Acknowledgments

Thanks go to Michael Wynn, Sarah Vial, and Prakash Prabhakar for the generous supply of protein kinases used in this study. The authors gratefully acknowledge Scott Raybuck for critiquing the manuscript and providing his support during this research.

References

[1] G. Manning, D.B. Whyte, R. Martinez, T. Hunter, S. Sudarsanam, The protein kinase complement of the human genome, Science 298 (2002) 1912–1934.
[2] R.V. Bhat, S.L. Budd Haeberlein, J. Avila, Glycogen synthase kinase 3: A drug target for CNS therapies, J. Neurochem. 89 (2004) 1313–1317.
[3] Z. Chen, F.Y. Lee, K.N. Bhalla, J. Wu, Potent inhibition of platelet-derived growth factor-induced responses in vascular smooth muscle cells by BMS-354825 (dasatinib), Mol. Pharmacol. 69 (2006) 1527–1533.
[4] K. Garber, The second wave in kinase cancer drugs, Nat. Biotechnol. 24 (2006) 127–130.
[5] B.M. Klebl, G. Muller, Second-generation kinase inhibitors, Expert Opin. Ther. Targets 9 (2005) 975–993.
[6] J.J. Ventura, A.R. Nebreda, Protein kinases and phosphatases as therapeutic targets in cancer, Clin. Transl. Oncol. 8 (2006) 153–160.

[7] J.A. Landro, I.C. Taylor, W.G. Stirtan, D.G. Osterman, J. Kristie, E.J. Hunnicutt, P.M. Rae, P.M. Sweetnam, HTS in the new millennium: The role of pharmacology and flexibility, J. Pharmacol. Toxicol. Methods 44 (2000) 273–289.
[8] J. Yong, C.M. Quinn, A.I. Gagnon, R. Talanian, Homogeneous time-resolved fluorescence and its applications for kinase assays in drug discovery, Anal. Biochem. 356 (2006) 273–281.
[9] M. Huse, J. Kuriyan, The conformational plasticity of protein kinases, Cell 109 (2002) 275–282.
[10] D.A. Johnson, P. Akamine, E. Radzio-Andzelm, M. Madhusudan, S.S. Taylor, Dynamics of cAMP-dependent protein kinase, Chem. Rev. 101 (2001) 2243–2270.
[11] N.M. Levinson, O. Kuchment, K. Shen, M.A. Young, M. Koldobskiy, M. Karplus, P.A. Cole, J. Kuriyan, A Src-like inactive conformation in the Abl tyrosine kinase domain, PLoS Biol. 4 (2006) e144.
[12] T. Schindler, W. Bornmann, P. Pellicena, W.T. Miller, B. Clarkson, J. Kuriyan, Structural mechanism for STI-571 inhibition of Abelson tyrosine kinase, Science 289 (2000) 1938–1942.
[13] G.A. Holgate, W.H.J. Ward, Measurements of binding thermodynamics in drug discovery, Drug Discov. Technol. 10 (2005) 1543–1550.
[14] I.J. Colton, J.D. Carbeck, J. Rao, G.M. Whitesides, Affinity capillary electrophoresis: A physical–organic tool for studying interactions in biomolecular recognition, Electrophoresis 19 (1998) 367–382.
[15] J. Oravcova, B. Bohs, W. Lindner, Drug–protein binding sites: New trends in analytical and experimental methodology, J. Chromatogr. B 677 (1996) 1–28.
[16] H. Nordin, M. Jungnelius, R. Karlsson, O.P. Karlsson, Kinetic studies of small molecule interactions with protein kinases using biosensor technology, Anal. Biochem. 340 (2005) 359–368.
[17] G.S. Van Aller, R. Nandigama, C.M. Petit, W.E. DeWolf Jr., C.J. Quinn, K.M. Aubart, M. Zalacain, S.B. Christensen, R.A. Copeland, Z. Lai, Mechanism of time-dependent inhibition of polypeptide deformylase by actinonin, Biochemistry 44 (2005) 253–260.
[18] C.W. Carreras, A. Schirmer, Z. Zhong, D.V. Santi, Filter binding assay for the geldanamycin–heat shock protein 90 interaction, Anal. Biochem. 317 (2003) 40–46.
[19] P. Kuzmic, M.L. Moss, J.L. Kofron, D.H. Rich, Fluorescence displacement method for the determination of receptor–ligand binding constants, Anal. Biochem. 205 (1992) 65–69.
[20] R. Zhang, T. Mayhood, P. Lipari, Y. Wang, J. Durkin, R. Syto, J. Gesell, C. McNemar, W. Windsor, Fluorescence polarization assay and inhibitor design for MDM2/p53 interaction, Anal. Biochem. 331 (2004) 138–146.
[21] W.X. Zhang, R. Wang, D. Wisniewski, A.I. Marcy, P. LoGrasso, J.M. Lisnock, R.T. Cummings, J.E. Thompson, Time-resolved Förster resonance energy transfer assays for the binding of nucleotide and protein substrates to p38α protein kinase, Anal. Biochem. 343 (2005) 76–83.
[22] R. Masui, S. Kuramitsu, Probing of DNA-binding sites of *Escherichia coli* RecA protein utilizing 1-anilinonaphthalene-8-sulfonic acid, Biochemistry 37 (1998) 12133–12143.
[23] S. Mizyed, A. Oddone, B. Byczynski, D.W. Hughes, P.J. Berti, UDP–*N*-acetylmuramic acid (UDP–MurNAc) is a potent inhibitor of MurA (enolpyruvyl–UDP–GlcNAc synthase), Biochemistry 44 (2005) 4011–4017.
[24] T. Kinoshita, M. Matsubara, H. Ishiguro, K. Okita, T. Tada, Structure of human Fyn kinase domain complexed with staurosporine, Biochem. Biophys. Res. Commun. 346 (2006) 840–844.
[25] W. Meng, L.L. Swenson, M.J. Fitzgibbon, K. Hayakawa, E. Ter Haar, A.E. Behrens, J.R. Fulghum, J.A. Lippke, Structure of mitogen-activated protein kinase-activated protein (MAPKAP) kinase 2 suggests a bifunctional switch that couples kinase activation with nuclear export, J. Biol. Chem. 277 (2002) 37401–37405.
[26] O. Futer, A.R. Saadat, J.D. Doran, S.A. Raybuck, S. Pazhanisamy, Phosphoryl transfer is not rate-limiting for the ROCK I-catalyzed kinase reaction, Biochemistry 45 (2006) 7913–7923.
[27] A. Kotlyarov, A. Neininger, C. Schubert, R. Eckert, C. Birchmeier, H.D. Volk, M. Gaestel, MAPKAP kinase 2 is essential for LPS-induced TNF-α biosynthesis, Nat. Cell Biol. 1 (1999) 94–97.
[28] Z.X. Wang, An exact mathematical expression for describing competitive binding of two different ligands to a protein molecule, FEBS Lett. 360 (1995) 111–114.
[29] Y. Liu, J. Jiang, P.L. Richardson, R.D. Reddy, D.D. Johnson, W.M. Kati, A fluorescence polarization-based assay for peptidyl prolyl *cis*/*trans* isomerase cyclophilin A, Anal. Biochem. 356 (2006) 100–107.
[30] S.M. Miick, S. Jalali, B.P. Dwyer, J. Havens, D. Thomas, M.A. Jimenez, M.T. Simpson, B. Zile, K.L. Huss, R.M. Campbell, Development of a microplate-based, electrophoretic fluorescent protein kinase A assay: Comparison with filter-binding and fluorescence polarization assay formats, J. Biomol. Screen. 10 (2005) 329–338.
[31] J.H. Zhang, T.D. Chung, K.R. Oldenburg, A simple statistical parameter for use in evaluation and validation of high throughput screening assays, J. Biomol. Screen. 4 (1999) 67–73.
[32] C. Pargellis, L. Tong, L. Churchill, P.F. Cirillo, T. Gilmore, A.G. Graham, P.M. Grob, E.R. Hickey, N. Moss, S. Pav, J. Regan, Inhibition of p38 MAP kinase by utilizing a novel allosteric binding site, Nat. Struct. Biol. 9 (2002) 268–272.
[33] J.L. Gross, W.F. Herblin, U.H. Do, J.S. Pounds, L.J. Buenaga, L.E. Stephens, Characterization of specific [^{3}H]dimethylstaurosporine binding to protein kinase C, Biochem. Pharmacol. 40 (1990) 343–350.